Chinese Journal of Polymer Science Vol. 34, No. 1, (2016), 1–12

Chinese Journal of Polymer Science

Improve the Thermal and Mechanical Properties of Poly(L-lactide) by Forming Nanocomposites with Pristine Vermiculite*

Hai-mu Ye**, Kai Hou and Qiong Zhou

Department of Materials Science and Engineering, Beijing Key Laboratory of Failure, Corrosion and Protection of Oil/Gas Facilities, China University of Petroleum, Beijing 102249, China

Abstract Poly(L-lactide) (PLLA)/pristine vermiculite nanocomposites were prepared by melt blending in a twin-screw extruder, and the detailed information of vermiculite dispersion state and effect of vermiculite on thermal and mechanical properties were systematically studied. The results show that the dispersion of vermiculite in the matrix is quite well when the loading content does not exceed 3 wt%. Pristine vermiculite can obviously improve the melt-crystallization temperature during the nonisothermal crystallization. Both crystallization time span and spherulitic size of PLLA decrease with the increasing amount of vermiculite under isothermal crystallization condition by enhancing the primary nucleation of PLLA. And the adding vermiculite can also improve the tensile modulus and Izod impact strength of PLLA. The intrinsic mechanism for the nucleating effect of vermiculite on PLLA is proposed to be the epitaxial crystallization and specific interaction between vermiculite and PLLA.

Keywords: Poly(L-lactide); Vermiculite; Crystallization behavior; Epitaxial crystallization; Nucleating agent.

INTRODUCTION

Nowadays polymer materials are playing increasingly important roles in our daily life, but in the meanwhile the accompanying environmental pollution by generous use of traditional polymer products has became one of the most serious problems facing mankind. Thus, research in biodegradable polymers has received increasing attention for their wide application in environmental protection and renewable feature. Among them, poly(L-lactide) (PLLA) is one of the most popular and important biodegradable polymers because it possesses comparable thermal and mechanical properties with commercial polyolefin materials[1]. However, the slow crystallization rate and low crystallinity of PLLA make it difficult to be processed by some traditional methods such as injection molding and restrict its practical application. Therefore, considerable efforts have been made to improve the crystallization behavior[2–4]. The most useful and effective way is to add nucleating agents to lower down the surface free energy barrier towards primary nucleation and initiate crystallization at higher temperatures upon cooling. There are many kinds of nucleating agents, including inorganic substances[5–8], small organic molecules[9–13], nanofillers[14–16], and polymeric materials[17–19], and studies are focus on finding new effective nucleating agents as well as their nucleation mechanism.

Vermiculite, like the well-known montmorillonite, belongs to the general family of layered silicates. This clay contains either Al^{3+} or Mg^{2+} and Fe^{2+} as normal octahedral ions, and a tetrahedral sheet in which Al^{3+} occurs as a substituted ion in place of some of the Si^{4+}. Compared with montmorillonite, vermiculite has good

* This work was financially supported by the National Natural Science Foundation of China (No. 21304108) and the Science Foundation of China University of Petroleum-Beijing (No. YJRC-2013-14, 2462013BJRC001).
** Corresponding author: Hai-mu Ye (叶海木), E-mail: yehaimu@cup.edu.cn
Received June 1, 2015; Revised August 20, 2015; Accepted August 23, 2015
doi: 10.1007/s10118-016-1724-5

crystallinity, mineral purity, abundant resources and other advantages. It was reported that vermiculite could be used to improve performance of different polymer matrices, such as, mechanical properties enhancement in polypropylene/vermiculite nanocomposites and polyamide-6/vermiculite nanocomposites[20, 21], gas barrier properties improvement in butyl rubber/vermiculite nanocomposites[22]. Organic modified vermiculite (OVMT) has also been used to blend into PLLA matrix and the relevant properties were investigated[23, 24]. The crystallization behavior of PLLA was not obviously enhanced after the addition of OVMT. However, the length of vermiculite *a* axis is 0.530 nm[25], which is just half of *a* axis of PLLA α-form crystal[26]. The good lattice matching may suggest PLLA chains could easily epitaxially crystallize on pristine vermiculite surface. Therefore, the aim of this work was to study the effect of pristine vermiculite on the thermal and mechanical properties of PLLA and the nucleation mechanism.

EXPERIMENTAL

Materials and Blend Preparation

Commercial PLLA with a stereoisomer composition of 1.2 mol%−1.6 mol% D-isomer lactide (PLA-4032D) was supplied by NatureWorks® LLC (USA). The number-average molecular weight (M_n) and the polydisperse index (PDI) are 1.34×10^5 g/mol and 1.86, respectively. The vermiculite with millimeter level sheet shape was produced by Lingshou Mineral Processing Plant, it was milled in a ball-mill to transform into fine powder (~ 2 μm in size) and then treated at 300 °C for 12 h.

Before blending, PLLA was dried in vacuo at 50 °C for 12 h. PLLA blends with desired amounts of vermiculite were prepared by melt mixing with a Thermo Scientific Process 11 twin-screw extruder at 50 r/min and 190 °C. The mixing compositions of vermiculite were 1 wt%, 3 wt%, 5 wt% and 10 wt%. The neat PLLA specimen was also processed with the same extrusion condition to serve as blank. The blends were denoted as PLLA*x*, *x* represented the weight percentage of vermiculite in specimen. Then the resulting materials were granulated and injection molded by using a Thermo Scientific HAAKE MiniJet machine at 190 °C to obtain the tensile splines and impact splines.

Characterization

The dispersion state of vermiculite in PLLA matrix was observed by an FEI F20 transmission electron microscope (TEM). The cross-section morphologies of cryo-fractured and impact-fractured splines were examined using a Quanta 200F field emission scanning electron microscope (SEM). Before SEM examination, the cross section was coated with ultrathin Au film in a high vacuum turbo evaporator to enhance the surface conductivity. The spherulitic morphologies of different specimens were captured on a Leica DM2500P polarized optical microscope (POM) equipped with a Linkam THMS600 hot stage.

A NETZSCH 204 F1 instrument equipped with an intercooler as cooling system was used to measure the non-isothermal and isothermal crystallization behavior of all specimens. The instrument was calibrated in temperature and in enthalpy with indium as standard specimen. Dry argon was used as purge gas at a rate of 60 mL/min. The non-isothermal procedure was as follows: the specimen was first heated from 20 °C to 190 °C and held for 5 min to eliminate the previous thermal history, then cooling down to 20 °C at a cooling rate of 5 K/min, finally, second heating scan was carried out from 20 °C to 190 °C at a heating rate of 10 K/min. The degree of crystallinity (X_c) of each specimen was calculated considering the melting enthalpy of 100% crystalline PLLA as 93 J/g[27]. Wide angle X-ray diffraction (WAXD) measurements were performed at ambient condition on a Bruker AXS D8 instrument using a graphite-filtered Cu Kα radiation target (λ_{Cu} = 0.15405 nm). Data were collected in the 2θ interval from 5° to 35° with a scan rate of 2 (°)/min. Fourier transform infrared (FTIR) spectra were recorded on a Bruker Tensor II spectrometer under the ATR mode by signal averaging over 32 scans at a resolution of 4 cm^{-1} in the wavenumber range of 4000–400 cm^{-1}. The molecular weights (M_n and M_w) of specimens were determined by a Viscotek-M302 TDA multiple testing gel chromatography system, the measurements were carried out at 40 °C with a Shimadzu GPC−804C column at a flow rate of 1.0 mL/min. Chloroform was used as the eluent, and Fluka polystyrene standards were used to obtain the calibration curve.

Tensile measurements were carried out on a WDL-5000N electronic universal tensile machine at 25 °C, and the drawing dumbbell spline was in a shape of 75 mm (length) × 4 mm (width) × 1.2 mm (thickness). The tensile rate was set as 10 mm/min. Notched impact strength of specimens were tested with 2.5 mm V-notch depth using a Jinjian XJUD-5.5 Izod impact machine. Five splines were tested to obtain an average value for each specimen. Dynamic mechanical analysis (DMA) was performed on an Anton Parr MCR301 stress/strain controlled rheometer from 20 °C to 120 °C at a heating rate of 3 K/min, a strain of 0.2% and a frequency of 1 Hz in the torsional configuration.

RESULTS AND DISCUSSION

Dispersion of Vermiculite

Dispersion state of filler displays great influence on various properties of the composites, therefore TEM was employed to reveal the state of vermiculite in PLLA matrix. Representative micro morphologies of vermiculite fragments in different specimens after blending are shown in Fig. 1. It could be found that vermiculite was crushed and delaminated to small flakes after the melt extrusion processing and the adding content of vermiculite showed obvious influence on the dispersion state. In PLLA1 and PLLA3, vermiculite was well separated and no agglomeration appeared, vermiculite flakes presented as lamellar structure with side length around 100 nm. With more adding vermiculite, *i.e.* in PLLA5 and PLLA10 the crushing degree of vermiculite decreased or the vermiculite fragments tended to agglomerate, resulting in some lager and thicker grain granules. So during the twin-screw extrusion process, vermiculite was easily transformed from the initial micrometer-scale size to the nanoscale size, while the transformation could not be fully realized with more addition of vermiculite probably due to limited energy input. Longer blending time might lead to better dispersion state and smaller size.

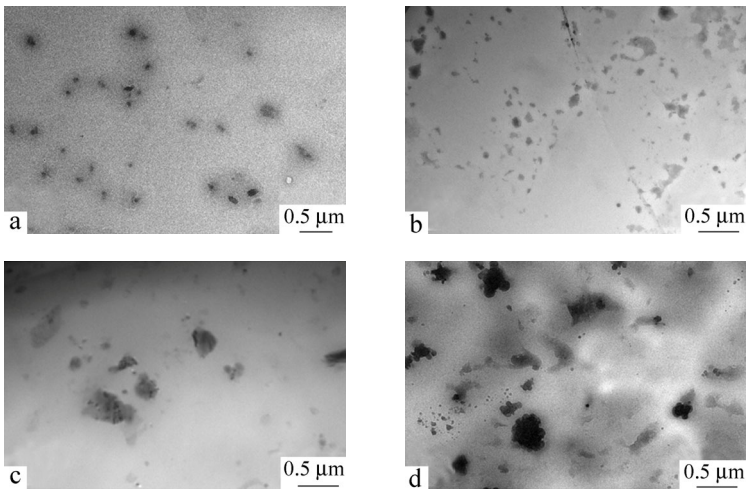

Fig. 1 Representative TEM images of PLLA/vermiculite composites: (a) PLLA1, (b) PLLA3, (c) PLLA5 and (d) PLLA10

Crystallization Behavior

Figure 2 shows the X-ray diffractograms of neat vermiculite, neat PLLA and PLLA/vermiculite composites with different vermiculite loading contents. Neat PLLA and PLLA/vermiculite composites were prepared by natural cooling from molten state at 190 °C. The vermiculite exhibited two characteristic diffraction peaks at 2θ of 8.78° (d = 1.006 nm) and 26.61° (d = 0.335 nm), which are corresponding to the (001) and (003) lattice planes, respectively. The diffractogram of PLLA showed a large bulge superimposing with a small diffraction peak, indicating the neat PLLA was almost amorphous. And the diffraction peaks belonging to PLLA crystals became more and more intense with increasing content of vermiculite. The arising diffraction peaks at 2θ of 14.82°, 16.71°, 19.06° and 22.37° revealed that vermiculite could enhance the formation of α-form PLLA crystals. Diffraction peaks belonging to vermiculite still remained in composites, and the corresponding 2θ positions kept

the same as initial vermiculite. The unaltered interplanar spacing of the basal plane revealed that PLLA chains did not intercalate the interlayers. Thus vermiculite was split into thinner layered structure during blending process, while no PLLA chains intercalation behavior happened. The enhancement of PLLA crystallization should result from the introduction of vermiculite surface.

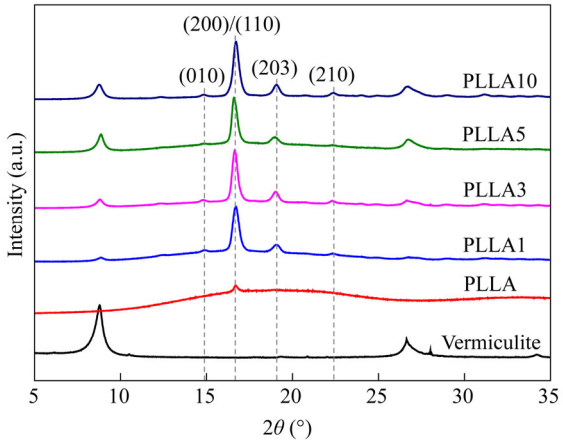

Fig. 2 The wide angle X-ray diffractograms of vermiculite, PLLA and PLLA/vermiculite composites

In order to investigate detailed effect of vermiculite on the crystallization of PLLA, both nonisothermal and isothermal crystallization behavior were analyzed by DSC. Figure 3(a) shows the melt-crystallization DSC curves of neat PLLA and PLLA composites at a cooling rate of 5 K/min after melting at 190 °C for 5 min. No crystallization peak but a clear glass transition was detected for neat PLLA during the cooling process, which should be stemmed from the poor polymer chains diffusion and nucleation ability. The resultant specimen was completely amorphous. With 1 wt% vermiculite adding into the PLLA matrix, an obvious crystallization temperature (T_c) appeared at 97.5 °C, and the change of heat capacity during glass transition lowered down, indicating vermiculite could play as effective nucleating agent for PLLA. The T_c and crystallization enthalpy increased with increasing vermiculite content, and the thermal parameters of specimens are tabulated in Table 1. T_c value reached 100.7 °C for PLLA3 and further slightly increased to 102.8 °C for PLLA10. Figure 3(b) shows the subsequent melting processes of all specimens. Both PLLA and PLLA1 exhibited cold crystallization phenomenon, the cold crystallization temperatures (T_{cc}) were 115.2 and 108.8 °C for PLLA and PLLA1, respectively. The lower shift of T_{cc} for PLLA1 comparing with neat PLLA confirmed the accelerating ability of vermiculite on PLLA crystallization behavior. With more adding vermiculite, the cold crystallization peak disappeared, which was the result of fully melt-crystallization during the previous cooling process. The overall melting enthalpy increased from 0 for neat PLLA to ~32 J/g for PLLA composites with vermiculite more than 3 wt%, and the corresponding normalized relative crystallinity increased from 0% to ~34%.

Table 1. Glass transition temperature (T_g), crystallization temperature (T_c), cold crystallization temperature (T_{cc}), melting temperature (T_m), overall melting enthalpy ($\Delta H_m - \Delta H_{cc}$), and the relative crystallinity (X_c) of neat PLLA and PLLA composites

Specimen	T_g (°C)	T_c (°C)	T_{cc} (°C)	T_m (°C)	$\Delta H_m - \Delta H_{cc}$* (J/g)	X_c
PLLA	62.0	–	115.2	167.6	0	0
PLLA1	62.1	97.5	108.8	168.1	20.4	21.8%
PLLA3	63.4	100.7	–	168.7	31.9	34.1%
PLLA5	64.3	100.8	–	168.5	32.5	34.7%
PLLA10	63.3	102.8	–	169.4	31.8	34.0%

* The overall melting enthalpy was obtained by dividing apparent measured values to the weight percentage of PLLA in composites.

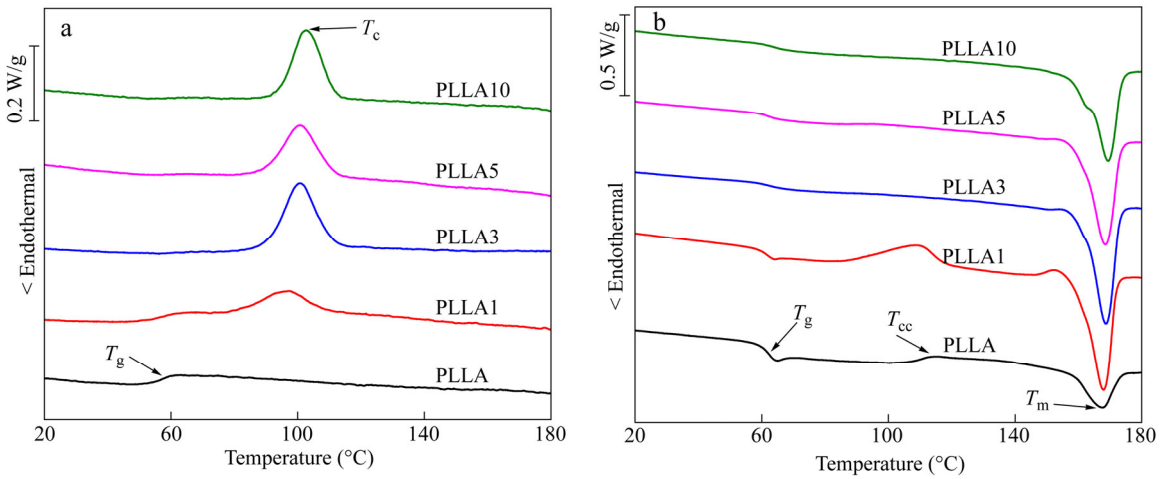

Fig. 3 (a) Melt-crystallization DSC curves of neat PLLA and PLLA composites with different addition amounts of vermiculite at a cooling rate of 5 K/min, and (b) the subsequence heating process at a rate of 10 K/min

To further qualify the nucleating ability of vermiculite on PLLA matrix, isothermal crystallization kinetics of neat PLLA and PLLA composites was investigated. Figure 4(a) shows the DSC curves of different specimens isothermally crystallized at 120 °C. Obviously, at such supercooling degree, the crystallization rate of neat PLLA was rather low; it took longer than 80 min before finishing the total crystallization process. When 1 wt% vermiculite was introduced, the crystallization time was sharply shortened to around 12 min, and further shortened with more vermiculite contents. The crystallization time span was only about 5 min for PLLA10, which was just one-sixteenth of that for neat PLLA. The relative crystallinity (X_t) at a given time (t) could be obtained from the integrated area of the DSC curve from $t = 0$ to t divided by the integrated area of the whole exothermal curve. A horizontal line from a point after the crystallization exotherm was used as the baseline for integration, and then the typical sigmoid shape conversion curves of X_t versus t can be attained. Figure 4(b) displays the X_t~t plotting of neat PLLA and PLLA composites isothermally crystallized at 120 ºC. Then the well-known Avrami equation[28–30] was employed to analyze the overall isothermal melt-crystallization kinetics of PBS. The equation is given as:

$$1 - X_t = \exp(-kt^n) \tag{1}$$

where n is the Avrami exponent related to nucleation mechanism (homogeneous or heterogeneous) and growth dimension of crystal, k is the overall rate constant composed of nucleation and growth part. The logarithmic form of Eq. (1) can be rearranged as:

$$\lg[-\ln(1 - X_t)] = \lg k + n \lg t \tag{2}$$

The crystallization parameters n and k can be obtained from the intercept and slope by linear fit of $\lg[-\ln(1-X_t)]$ versus $\lg t$ (Fig. 4c). All fits were performed for a relative crystallinity range encompassing 3%–20% to minimize the experimental error[31], such as, the equipment sensitive in the very early crystallization stage and the impingement between spherulites in the late crystallization stage. The correlation coefficients of the plot fit (R^2) for all specimens are larger than 0.99. For comparion, n, k, and crystallization half-time ($t_{1/2}$) are summarized in Table 2. The calculated Avrami exponents (n) for specimens were all close to 2, suggesting two-dimensional mode with heterogeneous nucleation growth behavior for all specimens. The addition of vermiculite did not change the spatial growth behavior of PLLA, while the overall crystallization rate constant increased significantly. The total crystallization growth rates, reciprocal of crystallization half-time ($t_{1/2}^{-1}$), for PLLA composites were much higher than that for neat PLLA. The $t_{1/2}^{-1}$ values of PLLA3 and PLLA10 were about eleven and seventeen times of $t_{1/2}^{-1}$ of neat PLLA, respectively. These were quantitative evidences for the effective nucleating effect of vermiculite on PLLA.

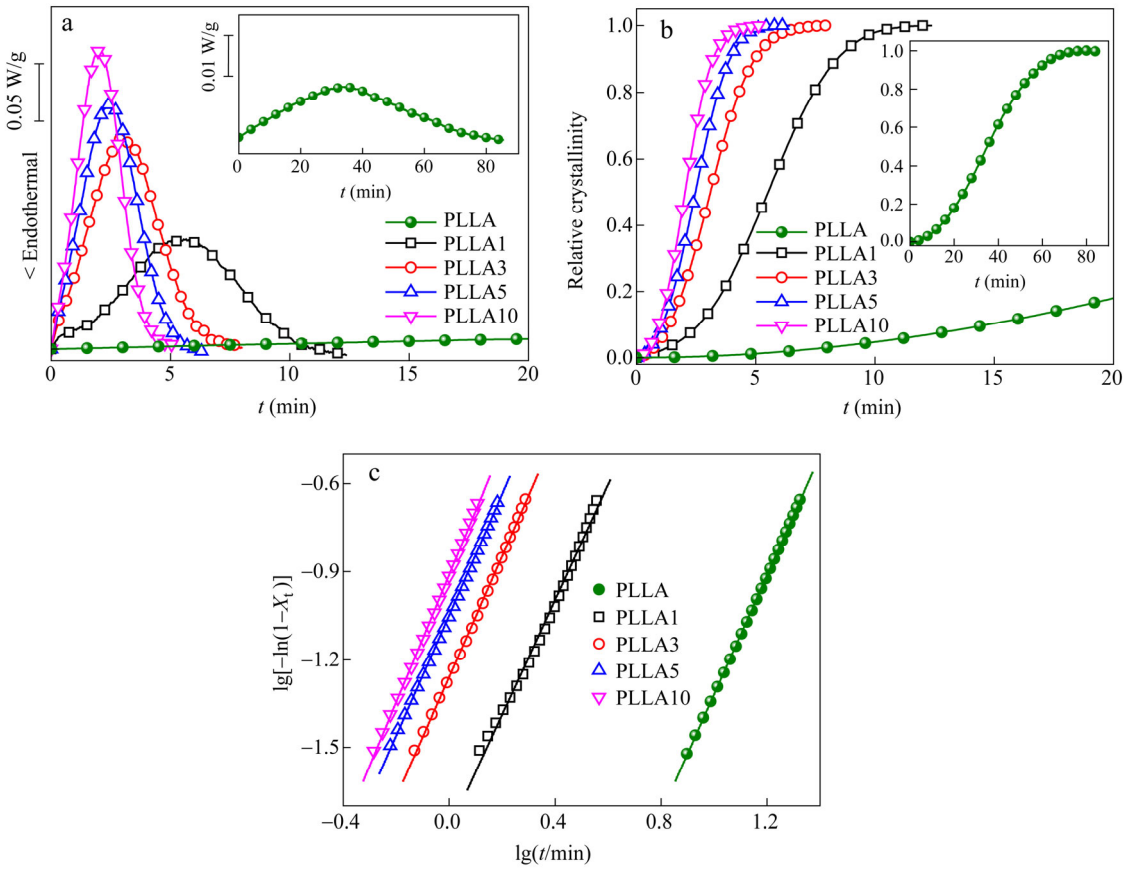

Fig. 4 (a) The DSC curves, (b) development of relative crystallinity with crystallization time, and (c) plotting of lg[−ln(1−X_t)] versus lg$t$ of neat PLLA and PLLA composites isothermally crystallized at 120 °C

Table 2. Avrami parameters of neat PLLA and PLLA composites at 120 °C

Specimen	n	k (min^{-n})	$t_{1/2}$ (min)	R^2
PLLA	2.03	4.43×10^{-4}	37.46	0.999
PLLA1	1.96	1.66×10^{-2}	6.71	0.994
PLLA3	2.06	5.51×10^{-2}	3.42	0.999
PLLA5	2.06	8.95×10^{-2}	2.70	0.999
PLLA10	2.18	1.23×10^{-1}	2.21	0.999

Furthermore, effect of vermiculite on the spherulitic morphology of PLLA was also studied by POM, as shown in Fig. 5. The spherulitic diameter of neat PLLA isothermally crystallized at 95 °C was about 300 μm, and it decreased to about 120 μm when 1 wt% vermiculite was blended in. And the spherulitic size of PLLA became smaller with more introducing vermiculite, such as spherulites in PLLA3 and PLLA5. The results demonstrated vermiculite served as effective nucleating agent and promoted the primary nucleation of PLLA matrix significantly.

Mechanical Properties

For semicrystalline polymers, crystallization has direct effects on the mechanical properties including tensile strength and Izod impact strength, because crystallinity, the orientation and size of crystals are all relevant to the macroscopic mechanical properties. Therefore, it is useful to know the effects. Dynamic mechanical analysis (DMA) is a useful and sensitive method to investigate the microstructure of the macromolecular chains conformations and movements during the exposure of polymers to a variety of temperatures by measuring the storage modulus (E') and loss modulus (E''). Figure 6 presents the storage modulus and loss modulus of neat

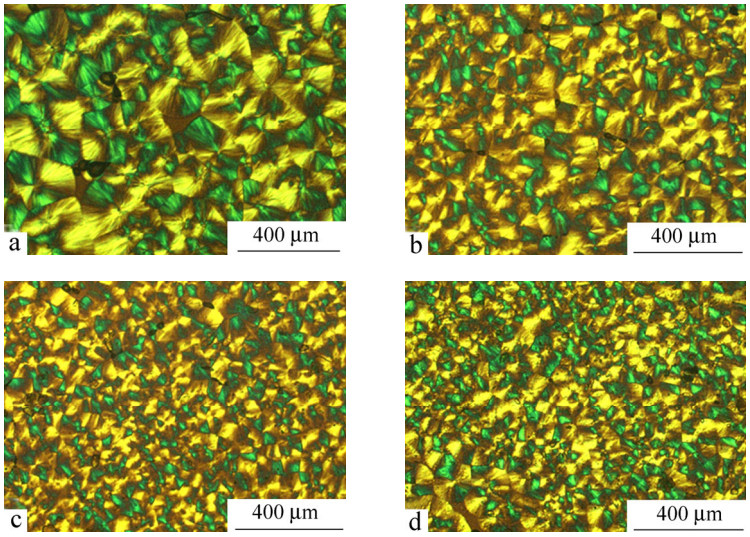

Fig. 5 POM micrographs of neat PLLA and PLLA/vermiculite composites: (a) PLLA, (b) PLLA1, (c) PLLA3 and (d) PLLA5

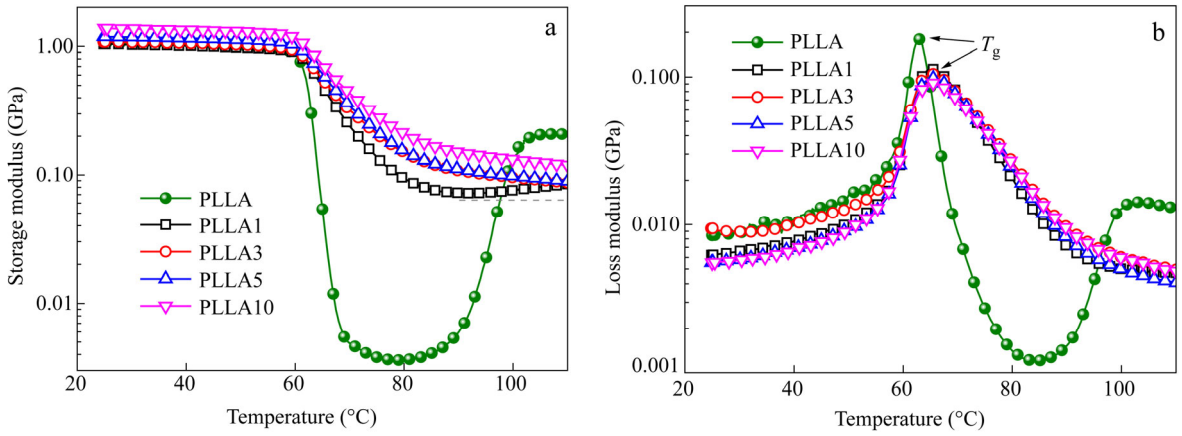

Fig. 6 Dynamic mechanical analysis curves of neat PLLA and PLLA/vermiculite composites: (a) storage modulus and (b) loss modulus

PLLA and PLLA composites as a function of temperature. The stroage modulus of all specimens remained stable till 60 °C and increased slightly with increasing vermiculite content; then the storage modulus decreased at temperatures close to glass transition temperature due to the great ehnacement of chain segment mobility. However, after this temperature range, storage modulus of neat PLLA increased obviously again with increasing temperature. The increase could be attributed to the cold crystallization behavior of PLLA. Also a similar but less apparent phenomenon could be seen in PLLA1. With higher vermiculite contents, the reincreasing behavior of storage modulus disappeared, indicating no cold crystallization behavior happened. A lot of alternations between neat PLLA and PLLA/vermiculite composites were also recorded in loss modulus curves (Fig. 6b). Neat PLLA was found to show a T_g at 62.8 °C, while the temperature shifted to higher values in case of composites. The increase of PLLA T_g in composites might be due to specific interaction, for instant, possible hydrogen-bonding between PLLA chains and vermiculite surface, and the mobility restriction of chain segments in the interphase between amorphous regions and crystal regions with raising crystallinity. Similar phenomena of increasing T_g have also been reported in PLLA composites with other fillers, such as multi-wall carbon nanotubes[32], and clay[33]. Furthermore, the loss modulus of PLLA composites displayed broader and lower

peaks during glass transition, implying the polymer chains were under some restrained conditions compraed with neat PLLA.

Figure 7 shows the typical stress-strain curves of neat PLLA and PLLA composites, all specimens displayed hard-brittle character. The mechanical properties of neat PLLA and PLLA composites during tensile process are listed in Table 3. Vermiculite added into PLLA could enhance the tensile modulus of specimens from 1.70 GPa to 2.00 GPa with the vermiculite content increasing from 0 wt% to 10 wt%. The specimens for tensile test were prepared under the same condition, naturally cooling to room temperature after melt-molding. Thus, the increasing tensile modulus should be attributed to the enhancing crystallinity and/or some probable interaction between vermiculite and PLLA matrix in composites. However, the composites still behaved as brittle material like neat PLLA, whose tensile strength is sensitive to the value of elongation at break. The tensile strength of PLLA/vermiculite composites was somewhat lower than that of neat PLLA, and the elongation at break of composites was smaller than that of neat PLLA too. The decrease in elongation at break should be owing to the hardening effect of vermiculite on PLLA matrix, and resulted in the slightly lower down of tensile strength for composites during testing. Similar phenomenon for PLLA composites with higher crystallinity but lower tensile strength compared with neat PLLA has also been reported in literature. Such as, PLLA/expanded graphite composites[34], PLLA/exfoliated graphite nanocomposites[35], and PLLA/hydroxyapatite composites[36]. Table 4 shows the molecular weights of as-received PLLA and processed PLLA in different specimens. While the molecular weight decreased due to the thermal degradation, vermiculite seems to display slight acceleration on the degradation degree of PLLA matrix. The smaller molecular weight for PLLA in composites might be another reason for the decrease of elongation at break, which leads to the lower down of tensile strength. On the other hand, the Izod impact strength increased first when vermiculite was introduced into PLLA, and reached 11.79 J/m for PLLA3, 27% higher than that of neat PLLA. Then the Izod impact strength slightly deteriorated with further more vermiculite content, which was in accordance with the TEM results. Some larger and thicker grain granules that might play a defect role in composites appeared in PLLA5 and PLLA10. The SEM images of cryo-fractured surface and impact-fractured surface for neat PLLA and PLLA composites are presented in Fig. 8. Both cryo- and impact-fractured surfaces were rather smooth for neat PLLA, revealing the brittle essence of PLLA. On the contrary, the surface morphologies became rough in composites and the roughness increased with increasing vermiculite. Especially, there appeared some fibrous structure, indicated by arrows, in cryo-fractured PLLA3 and all impact-fractured PLLA composites. These unique morphologies should be conducive to the display of higher Izod impact strength for composites compared with neat PLLA and the highest Izod impact strength for PLLA3 among all specimens. No aggregation of vermiculite was observed in the SEM images of PLLA composites also suggested the good dispersion of vermiculite in composites.

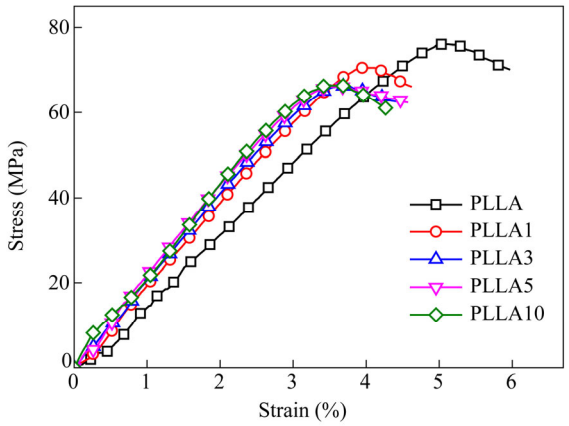

Fig. 7 Tensile stress-strain curves of neat PLLA and PLLA composites

Table 3. Mechanical properties of neat PLLA and PLLA composites at 25 °C

Specimen	Tensile modulus (GPa)	Tensile strength (MPa)	Elongation at break (%)	Izod impact strength (J/m)
PLLA	1.70 ± 0.02	73.52 ± 2.05	6.04 ± 0.2	9.26 ± 0.24
PLLA1	1.82 ± 0.02	69.78 ± 1.11	4.67 ± 0.1	11.27 ± 1.26
PLLA3	1.90 ± 0.07	64.69 ± 1.13	4.70 ± 0.3	13.79 ± 0.69
PLLA5	1.95 ± 0.06	66.03 ± 1.81	4.78 ± 0.2	11.05 ± 0.51
PLLA10	2.00 ± 0.13	66.17 ± 1.17	4.54 ± 0.4	11.56 ± 1.39

Table 4. Number-average molecular weights (M_n) and polydisperse indices (PDI) of as-received PLLA (as-PLLA) and PLLA specimens after processing

Specimen	as-PLLA	PLLA	PLLA1	PLLA3	PLLA5	PLLA10
M_n (g/mol)	1.34×10^5	1.05×10^5	0.97×10^5	0.86×10^5	0.91×10^5	0.88×10^5
PDI	1.86	1.49	1.65	2.85	2.37	1.98

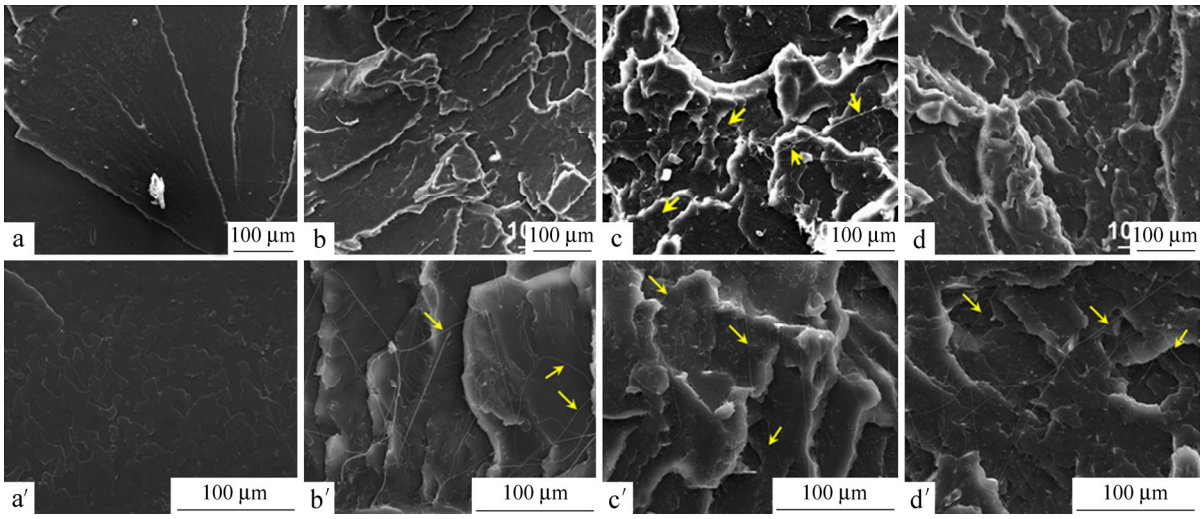

Fig. 8 SEM images of (top row) the cryo-fractured surface and (down row) the impact-fractured surface of different PLLA/vermiculite composites: (a) and (a′) neat PLLA, (b) and (b′) PLLA1, (c) and (c′) PLLA3, (d) and (d′) PLLA5

Discussion

Summarizing the experimental results, vermiculite showed obvious influence on the crystallization behavior and mechanical properties of PLLA. For crystallization behavior, DSC measurements and POM observations revealed that the incorporated vermiculite played as an effective nucleating agent for PLLA, thus facilitated the crystallization process of the matrix, improved the crystallinity, greatly shortened crystallization time, and decreased the spherulitic size of PLLA. In terms of mechanical properties, although the elongation at break and tensile strength for composites were slightly smaller than those of neat PLLA, the tensile modulus and Izod impact strength increased after introducing vermiculite. The Izod impact strength reached the maximum value when the vermiculite content was 3 wt%.

Here we try to interpret the mechanism of the ability of pristine vermiculite on nucleating PLLA. Presently, two mainly fundamental interpretations have been proposed as the mechanism for nucleating agent, the chemical nucleation[37] and the epitaxial nucleation[38]. As to the former, it is usually found in organic nucleator nucleated matrix where reaction occurs between nucleator and matrix. While in PLLA/vermiculite composites, there have no possible reaction could happen between PLLA and vermiculite during the preparation process according to their chemical structure. Thus, the possibility of chemical nucleation mechanism can be excluded. For epitaxial crystallization mechanism, it needs to have good lattice matching between matrix and additive. PLLA α form crystal adopts orthorhombic structure with parameters of a = 1.060 nm, b = 0.610 nm and c = 2.880 nm[26]. The unit cell parameters for vermiculite are a = 0.530 nm, b = 0.920 nm and c = 0.960 nm[25]. The c axis length of

vermiculite is not a fixed value and varies depending on the hydrated degree, for example, the *c* axis was detected as 1.006 nm in this study. The length of PLLA *a* axis is just twice of vermiculite *a* axis, and the length of PLLA *c* axis is close to threefold that of vermiculite *c* axis. The lattice matching provides the basic requirement for epitaxial crystallization of PLLA on vermiculite. Fernández *et al*. had carried out study on the properties of PLLA/organically modified vermiculite (OVMT) nanocomposites prepared by melt compounding, the accelerating ability of OVMT on PLLA crystallization was weaker than our study did, obvious cold crystallization behavior was observed for all composites during the second heating process in the study[23]. The cold crystallization behavior of PLLA was also found in PLLA-based copolymer/OVMT composites[24]. Although organic modification on vermiculite could benefit its exfoliation and dispersion in polymer matrix, the nucleating ability of vermiculite on PLLA was deteriorated. The reason came from absorption of organic molecules on the vermiculite surface, which resulted in the deterioration of lattice matching between PLLA matrix and vermiculite. Therefore, pristine vermiculite displays better nucleating ability than OVMT does.

In another aspect, does there exist specific interaction between PLLA and vermiculite? In order to enhance the possible interaction signal between PLLA and vermiculite, PLLA3 specimen was extracted with large amount of chloroform three times to remove the free PLLA, then the insoluble matter was separated through a centrifugal method with a centrifugal rate of 10000 r/min for 30 min and followed by a vacuum drying process at 30 °C for 48 h. The obtained specimen (marked as *e*PLLA3) was characterized using FTIR (Fig. 9). *e*PLLA3 showed a boarder FTIR absorption peak belonging to C=O stretching band at 1759 cm^{-1} coupling with a shoulder peak at 1776 cm^{-1}, which was quite different from the free amorphous PLLA showing a peak at 1755 cm^{-1} while similar to the crystallized PLLA. The absorption peak at 1759 cm^{-1} is a characteristic peak belonging to crystallization and has been attributed to the *gt* conformers in the lamellae phase and the interlamellar phase, and peak at 1776 cm^{-1} is connected with *gg* conformers in the interlamellar region, respectively[39, 40]. In addition, *e*PLLA3 did not exhibit the absorption peak 1749 cm^{-1}, revealing that polymer chains in *e*PLLA3 also did not take the exactly same conformation as crystallized PLLA. So it is plausibly that fractional PLLA chains in composites were absorbed to the vermiculite surface during the extrusion process with the aid of specific interaction (such as O—H···O=C hydrogen bonding or metallic cation-carbonyl), and the retention of a certain amount of PLLA on vermiculite after extraction process demonstrated the interaction is rather strong. The absorbed PLLA chains are forced to adopt *gt* conformers, which would be useful to induce the surrounding free PLLA chains to take the same conformation and lower down the entropic barrier during crystallization. In summary, both the lattice matching between PLLA and vermiculite and the *gt* conformers in absorbed chains would accelerate the crystallization of PLLA matrix. However, the question which plays as the major role is not clear, and further work will be carried out.

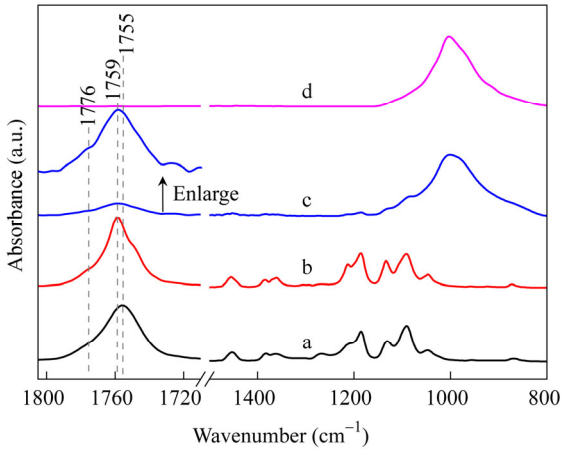

Fig. 9 FTIR spectra of (a) amorphous PLLA, (b) PLLA isothermally crystallized at 120 °C for 3 h, (c) *e*PLLA3 and (d) vermiculite (The amorphous PLLA was obtained by melt-quenched process from 190 °C to 4 °C.)

CONCLUSIONS

In this research, PLLA/vermiculite nanocomposites were prepared by melt blending in twin-screw extruder. The dispersion state of vermiculite in the matrix was quite well when the loading content does not exceed 3 wt%. The pristine vermiculite significantly facilitated the primary nucleation rate, and acted as effective nucleating agent for PLLA, leading to the sharp shortening of crystallization time. And the nucleation mechanism was attributed to epitaxial crystallization and specific interaction between vermiculite and PLLA. The adding vermiculite also improved the tensile modulus and Izod impact strength of PLLA.

REFERENCES

1 Chen, G.Q. and Patel, M.K., Chem. Rev., 2011, 112: 2082
2 Lim, L.T., Auras, R. and Rubino, M., Prog. Polym. Sci., 2008, 33: 820
3 Saeidlou, A., Huneault, M.A., Li, H. and Park, C.B., Prog. Polym. Sci., 2012, 37: 1657
4 Li, H. and Huneault, M.A., Polymer, 2007, 48: 6855
5 Ray, S.S., Pralay, M., Masami, O., Kazunobu, Y. and Kazue, U., Macromolecules, 2002, 35: 3104
6 Liao, R., Yang, B., Yu, W. and Zhou, C., J. Appl. Polym. Sci., 2007, 104: 310
7 Kolstad, J.J., J. Appl. Polym. Sci., 1996, 62: 1079
8 Pan, H. and Qiu, Z., Macromolecules, 2010, 43: 1499
9 Li, J., Chen, D., Gui, B., Gu, M. and Ren, J., Polym. Bull., 2011, 67: 775
10 Li, C. and Dou, Q., Thermochim. Acta, 2014, 594: e31
11 Tang, Z., Zhang, C., Liu, X. and Zhu, J., J. Appl. Polym. Sci., 2012, 125: 1108
12 Qiu, Z. and Li, Z., Ind. Eng. Chem. Res., 2011, 50: 12299
13 Weng, M., Qiu, Z., Thermochim. Acta, 2014, 577: 41
14 Zhao, Y., Qiu, Z. and Yang, W., J. Phys. Chem. B, 2008, 112: 16461
15 Wang, H. and Qiu, Z., Thermochim. Acta, 2011, 526: 229
16 Qiu, Z. and Guan, W., RSC Adv., 2014, 4: 9463
17 Schmidt, S.C. and Hillmyer, M.A., J. Polym. Sci., Part B: Polym. Phys., 2001, 39: 300
18 Pan, P., Shan, G. and Bao, Y., Ind. Eng. Chem. Res., 2014, 53: 3148
19 Zhao, Y. and Qiu, Z., RSC Adv., 2015, 5: 49216
20 Tjong, S.C., Meng, Y.Z. and Hay, A.S., Chem. Mater., 2002, 14: 44
21 Tjong, S.C., Meng, Y.Z. and Xu, Y., J. Polym. Sci., Part B: Polym. Phys., 2002, 40: 2860
22 Takahashi, S., Goldberg, H.A., Feeney, C.A., Karim, D.P., Farrell, M., O'Leary, K. and Paul, D.R., Polymer, 2006, 47: 3083
23 Fernández, M.J., Fernández, M.D. and Aranburu, I., Eur. Polym. J., 2013, 49: 1257
24 Fernández, M.J., Fernández, M.D. and Aranburu, I., Appl. Clay Sci., 2013, 80−81: 372
25 Williams-Daryn, S. and Thomas, R.K., J. Colloid Interf. Sci., 2002, 255: 303
26 Hoogsteen, W., Postema, A.R., Pennings, A.J., Brinke, G.T. and Zugenmaier, P., Macromolecules, 1990, 23: 634
27 Fisher, E.W., Sterzel, H.J. and Wegner, G., Kollid-Z Z Polym., 1973, 25: 980
28 Avrami, M.J., Chem. Phys., 1939, 7: 1103
29 Avrami, M.J., Chem. Phys., 1940, 8: 212
30 Avrami, M.J., Chem. Phys., 1941, 9: 177
31 Lorenzo, A.T., Arnal, M.L., Albuerne, J. and Müller, A.J., Polym. Test., 2007, 26: 222
32 Yoon, J.T., Jeong, Y.G., Lee, S.C. and Min, B.G., Polym. Adv. Technol., 2009, 20: 631
33 Krishnamachari, P., Zhang, J., Lou, J., Yan, J. and Uitenham, L., Int. J. Polym. Anal. Charact., 2009, 14: 336
34 Murariu, M., Dechief, A.L., Bonnaud, L., Paint, Y., Gallos, A., Fontaine, G., Bourbigot, S. and Dubois, P., Polym. Degrad. Stab., 2010, 95: 889

35 Kim, I.H. and Jeong, Y.G., J. Polym. Sci., Part B: Polym. Phys., 2010, 48: 850
36 Hong, Z., Zhang, P., He, C., Qiu, X., Liu, A., Chen, L., Chen, X. and Jing, X., Biomaterials, 2005, 26: 6296
37 Legras, R., Mercier, J.P. and Nield, E., Nature, 1983, 304: 432
38 Wittmann, J.C. and Lotz, B., Prog. Polym. Sci., 1990, 15: 909
39 Meaurio, E., López-Rodríguez, N. and Sarasua, J.R., Macromolecules, 2006, 39: 9291
40 Meaurio, E., Zuza, E., López-Rodríguez, N. and Sarasua, J.R., J. Phys. Chem. B, 2006, 110: 5790